Cocioabă *et al. EJNMMI Physics* (2025) 12:45
https://doi.org/10.1186/s40658-025-00755-2

EJNMMI Physics

YOUNG INVESTIGATORS Open Access

Optimized production of ^{89}Zr as a medical radioisotope on a variable energy cyclotron and external beam-line

Diana Cocioabă[1,2], Simona Baruta[1,3*], Liviu Crăciun[1], Radu Leonte[1], Andrei Necsoiu[1,2], Maria-Roxana Tudoroiu-Cornoiu[1,4], Alexandru Jipa[2] and Dana Niculae[1,5*]

*Correspondence:
Simona Baruta
simona.baruta@nipne.ro
Dana Niculae
dana.niculae@nipne.ro
[1]Radiopharmaceutical Research Centre, Horia Hulubei National Institute for Physics and Nuclear Engineering, Măgurele, Ilfov, Romania
[2]Doctoral School of Physics, Faculty of Physics, University of Bucharest, Măgurele, Ilfov, Romania
[3]Extreme Light Infrastructure – Nuclear Physics, Horia Hulubei National Institute for Physics and Nuclear Engineering, Măgurele, Ilfov, Romania
[4]Doctoral School of Applied Chemistry and Materials Science, Faculty of Chemical Engineering and Biotechnologies, National University of Science and Technology Politehnica Bucharest, Bucharest, Romania
[5]Faculty of Pharmacy, University of Medicine and Pharmacy Carol Davila, Bucharest, Romania

Abstract

Background Zirconium-89 (^{89}Zr) is a highly valued diagnostic radionuclide for positron emission tomography (PET) due to its long physical half-life of 78.4 h and decay characteristics, being preferred for the radiolabelling of nanoparticles and slow kinetics macromolecules, such as antibodies. ^{89}Zr-based high-resolution PET images can be employed to scan tumours and localize the tracer on a longer timeframe, which allows for real-time therapy monitoring. The goal of this study was to maximize the ^{89}Zr production yield by fine-tunning the irradiation parameters of a solid target, in two different experimental set-ups, using a variable energy 14–19 MeV TR-19 cyclotron. Monte Carlo programs simulated the irradiation geometry and estimated the activity and irradiation yields produced by the ^{89}Y(p, n)^{89}Zr reaction, at the process optimal parameters. The resulted data were compared with the experimental data collected in our particular irradiation setups.

Results ^{89}Zr was obtained from ^{nat}Y foil target using: (A) the solid target holder placed on the extraction port, and (B) the automated solid target irradiation station, installed on a sloped-down extension of the proton beamline. The two irradiation geometries are differentiated by the distances from the respective extraction ports, beam-geometry and shape, cooling capacity, and degrader's thickness. Based on the specific geometries, A and B, the Monte Carlo simulations output determined the optimal experimental irradiation parameters (extracted energy, degrader thickness, proton current intensity), as well as the target thickness. The 250 µm ^{nat}Y foils were irradiated with 14 MeV protons and an integrated current of 32 µA·h, on the solid target configuration A, and with 15.2 MeV protons, 100 µA·h on the solid target configuration B. After the dissolution and purification of the targets, [^{89}Zr]Zr-oxalate solutions of 1.28 ± 0.18 GBq, and 2.95 ± 0.31 GBq respectively, were evaluated, to determine the radionuclidic purity and contaminant levels of ^{89}Zr solutions across different incident proton beam energies. The pharmaceutical specifications require the solutions radionuclidic purity to be above 99.9% of the total radioactivity, as criteria of their suitability for use as radiopharmaceutical precursors for antibodies radiolabelling.

Conclusions Simulations were providing optimized input parameters to maximize the production yield of ^{89}Zr and subsequently, to achieve the highest possible activity with

no detriment to radionuclide purity, as per the [^{89}Zr]Zr-oxalate solution pharmaceutical specification. The parameters were then implemented in the experiments, and the production processes were tested on two particular irradiation configurations. The yields and activities produced through ^{89}Y(p, n)^{89}Zr reaction, at the TR-19 cyclotron were in good agreement with the simulations, within 18.4–21.3%, which include activity losses during irradiation and post-processing and uncertainties resulted from activity measurements and cross-section values.

Keywords Monte Carlo simulations, Proton irradiation, ^{nat}Y solid target, Variable energy cyclotron, Zirconium-89

Background

Over the last several years, positron emission tomography (PET) imaging involving ^{89}Zr radionuclide has presented an increased interest in nuclear medicine applications. Therefore, additional efforts are required to hasten the translation of ^{89}Zr-based tracers into clinical use. To successfully diagnose solid tumours by PET, the half-life of a radionuclide must be suitable for both stable target tissue accumulation and optimal biological elimination of the nonspecific bound radionuclide. The most commonly used PET radionuclides, such as ^{18}F and ^{11}C, have short half-lives of 109.7 min and 20 min, respectively, and are less sensitive for detecting solid tumours since they would undergo significant radioactive decay before reaching the tumours' centre [1]. Consequently, ^{89}Zr is becoming more and more interesting, particularly due to its half-life which is compatible with imaging using radiolabelled antibodies [2]. The radioisotope's ability to provide quantitative and high-resolution imaging is due to the β^+ emission branching ratio (22.8%) and low average positron energy (396 KeV) [3]. Although the gamma emission of 909 KeV, as it is shown in Fig. 1, is suboptimal for dosimetry, the longer half-life of ^{89}Zr (78.4 h), in comparison to the more commonly used ^{18}F (1.83 h), is advantageous in PET nuclear medicine studies to develop imaging agents that require longer acquisition times [4].

Zirconium-89 can be obtained by irradiating foils of natural yttrium mounted on an aluminum or copper disk, either via the ^{89}Y(p, n)^{89}Zr nuclear reaction or via the ^{89}Y(d,2n)^{89}Zr nuclear reaction. The chemistry of the separation of ^{89}Zr is the same regardless the production method. The aim of this work is to enhance the ability to produce ^{89}Zr by ^{89}Y(p, n) route, in highest yield and purity, by taking the advantages of a fine-tunning energy of TR-19 cyclotron, and carefully assessing the particular irradiation geometry, cooling capacity and target size. We compared the two existing experimental set ups, as alternative solutions. These set ups are allowing for different irradiating parameters and limitations. Monte Carlo simulation program is a very useful tool to plan the irradiation experiments, estimating the yield and activity produced, optimizing irradiation parameters, and particular geometries. Besides the energy on target, proton beam intensity and irradiation time, special attention need to be paid to the cooling capacity and beam shape, especially when the targets are installed on extensions of the proton beams. Target thickness is also important for the total yield, as the integrated energy delivered in the target is correlated with the total activity but also could induce potential radionuclide impurities. The validation of the parameters resulted from MC simulations is therefore mandatory before translation to a regular production.

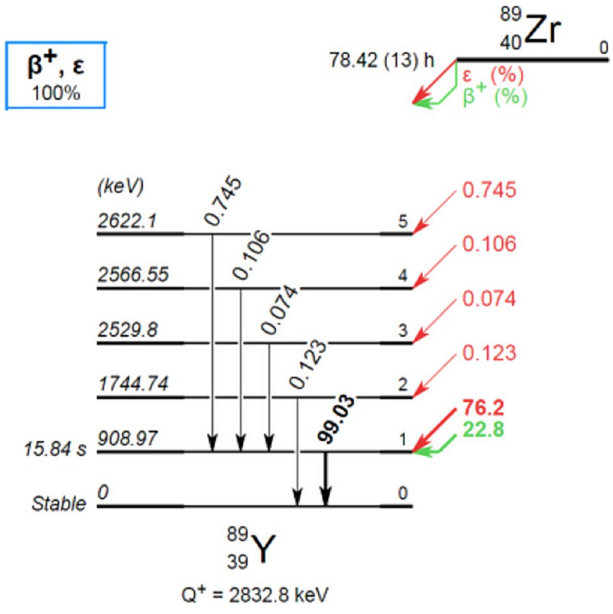

Fig. 1 Decay scheme of ^{89}Zr [5]

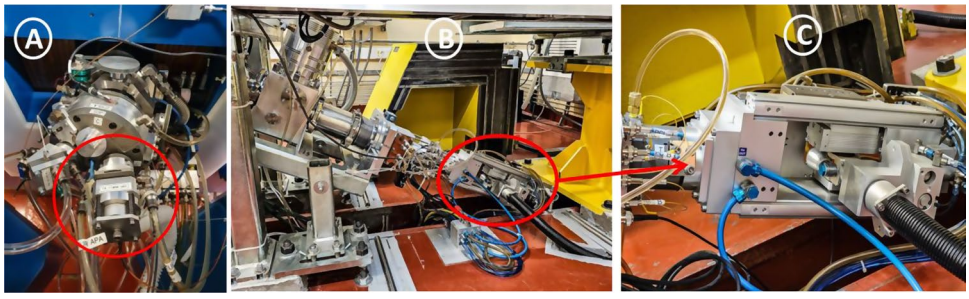

Fig. 2 TR-19 cyclotron set-ups: the solid target holder STH (**A**), the extension line of the proton beam (**B**) with the solid target irradiation unit STIU (**C**)

Methods

The experimental production of ^{89}Zr was achieved by irradiation of natural yttrium foils on the TR-19 cyclotron (Advanced Cyclotron Systems Inc., ACSI, Canada) [6] installed at the Radiopharmaceutical Research Centre (CCR), Horia Hulubei National Institute for Physics and Nuclear Engineering (IFIN-HH), Măgurele, Romania [7]. The extracted proton beam energy of the cyclotron is tunable in the 14–19 MeV range with a fine step of 100 keV. It can be degraded, if necessary, by Havar windows and aluminum foils [8]. Our facility provides two experimental setups to obtain ^{89}Zr via ^{89}Y(p, n)^{89}Zr nuclear reaction, by irradiation of thick natural yttrium foils: **(A)** on the Solid Target Holder (STH, ACSI, Canada) or **(B)** on the Solid Target Irradiation Unit (STIU, COMECER, Italy) [9] installed on the short proton beam extension line, slopeddown of the TR-19 cyclotron (Fig. 2). While the STIU is connected to the target preparation and post-processing purification station via a pneumatic transfer pipe, remotely controlled, the STH is loaded manually and unloaded pneumatically inside the bunker, in a dedicated lead container.

Prior to the experiments, simulations were run aiming to optimize the production yield of zirconium-89 and, thus, achieving the highest activity. The optimized parameters, as

resulted from the simulations, were subsequently used in the experiments. We considered the energy threshold for ^{89}Y(p, n)^{89}Zr reaction, the optimal thickness of the ^{nat}Y foil, the proton beam energy extracted/on-target, based on the energy loss distinctive for the experimental configurations, the maximum production yield and the maximum activity at the end of the bombardment (EOB).

The output results of the simulations were in good agreement with the experimental values of the zirconium-89 activity.

TALYS – cross sections simulation

TALYS is a software that simulates nuclear reactions and calculates the excitation functions in order to determine the optimal energy range [10]. The nuclear-reaction program shows the dependence of the nuclear cross-sections on the energy of the incident protons [11]. The excitation function was calculated to illustrate the zirconium-89 radionuclide formation via the ^{89}Y(p, n)^{89}Zr reaction. TALYS code [12] was used for target design, by calculating the theoretical cross sections for the possible nuclear reactions on yttrium-89 target (natural yttrium, 100% abundance ^{89}Y), in the 0–20 MeV range, as presented in Fig. 3a). Based on the calculations obtained with the TALYS code, we aimed to select the optimal energy range of the beam, between the target entrance and at the exit points, to get the highest activity high-purity zirconium-89. The main reaction has a threshold at 3.7 MeV and the maximum cross-section at around 13 MeV, proton beam energy. Two competing reactions are producing longer half-life zirconium-88 (83.4 day) via the (p,2n) reaction at a threshold energy of 13.076 MeV and yttrium-88 (106.6 days) via (p, pn) at a threshold energy of 11.609 MeV.

The ^{89}Y(p, pn)^{88}Y cross section is reported with a large error bar above the threshold to about 13 MeV. However, since the zirconium-89 solution for labelling is to be purified, the yttrium-88 contamination is not a major concern. On the contrary, the presence of zirconium-88 (half-life 83.4 days) in the final product can only be avoided by limiting the incident energy below 13 MeV, as reported by other studies. Observing the asymmetry of the curve representing the cross-section dependence on proton energy (Fig. 3a), and taking into account practical aspects such as the minimal extracted energy, the dissipation produced by degraders, and the thickness of commercially available Y-nat foils, the question is how much the incident energy can be increased to maximize the production capacity while keep the zirconium-88 amount within the accepted limits.

Also, the cross-sections for the reaction of interest (Fig. 3b), measured by different authors as provided in the EXFOR database are bearing quite high uncertainties and

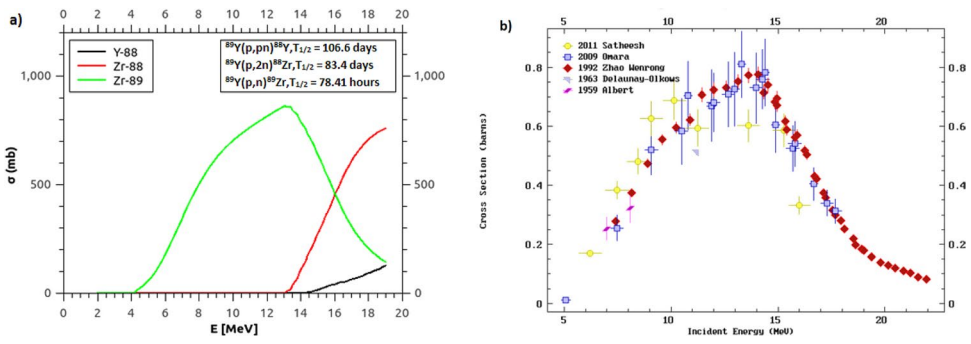

Fig. 3 Plots of the excitation function of the ^{89}Y(p, n)^{89}Zr nuclear reaction. **a**) The excitation function generated from the TALYS simulation package. **b**) The excitation function found in the EXFOR database [13]

significant differences, suggesting important influences of different experimental setups. However, the data agree the highest production yield is anticipated at 13 MeV, where the unwanted competing production of ^{88}Zr has the threshold. The ^{89}Y(p, n)^{89}Zr excitation function shows that the ^{89}Zr production exhibits good efficacy in the 8–15 MeV energy range. The output of the simulations should provide the extracted energy and the maximum energy on target surface, leading to high-quality zirconium-89 solution for radiolabelling, as per requirements for pharmaceutical use. It is also expected to give robust and reliable estimation of the yield and activity produced under specific experimental set-up (in particular, the installation of the target on the slope-down, 1.60 m proton beam extension).

SRIM/TRIM calculations

The Stopping and Range of Ions in Matter (SRIM) is a software package used to calculate the energy loss in matter. The program simulates charged particle range in different targets, particularly particle-solid interactions, using the Monte Carlo methods [14]. It has two primary programs: Tables of Stopping and Range of Ions in Simple Targets and Transport of Ions in Matter (TRIM) [15].

When choosing an yttrium target for the production of ^{89}Zr through proton irradiation on a cyclotron, the target's thickness plays a crucial role in determination of the balance between total activity and specific activity. We ran several simulations using the TRIM program to find the most suitable ^{nat}Y foil thickness, among the commercially available dimensions. We considered for the simulations the proton beam's energy of 12.9 MeV at the target's entrance, as represented in Fig. 4.

The emergent proton beam energy through varying thickness yttrium foils was calculated using TRIM. Figure 5 shows the energy loss in five different ^{89}Y foil thicknesses, represented by the 2 purple lines that delimit the energy range that passes through the target (the proton energy at the entrance and exit of the target, respectively). A thicker target would result in a higher total activity, as the AUC is higher for Fig. 5e), compared to the thinner ones. The specific activity (MBq/μg_{target}) has to be taken into account, the ideal balance between total activity and specific activity being clearly shown in Fig. 5d), corresponding to the 250 μm thickness. A high total activity ensures that sufficient

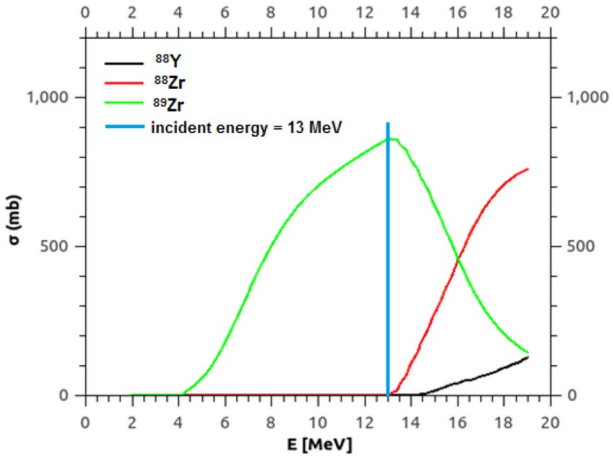

Fig. 4 Incident proton beam energy according to the cross-section of the radionuclide of interest (^{89}Zr) and potential radionuclide impurities (^{88}Zr and ^{88}Y)

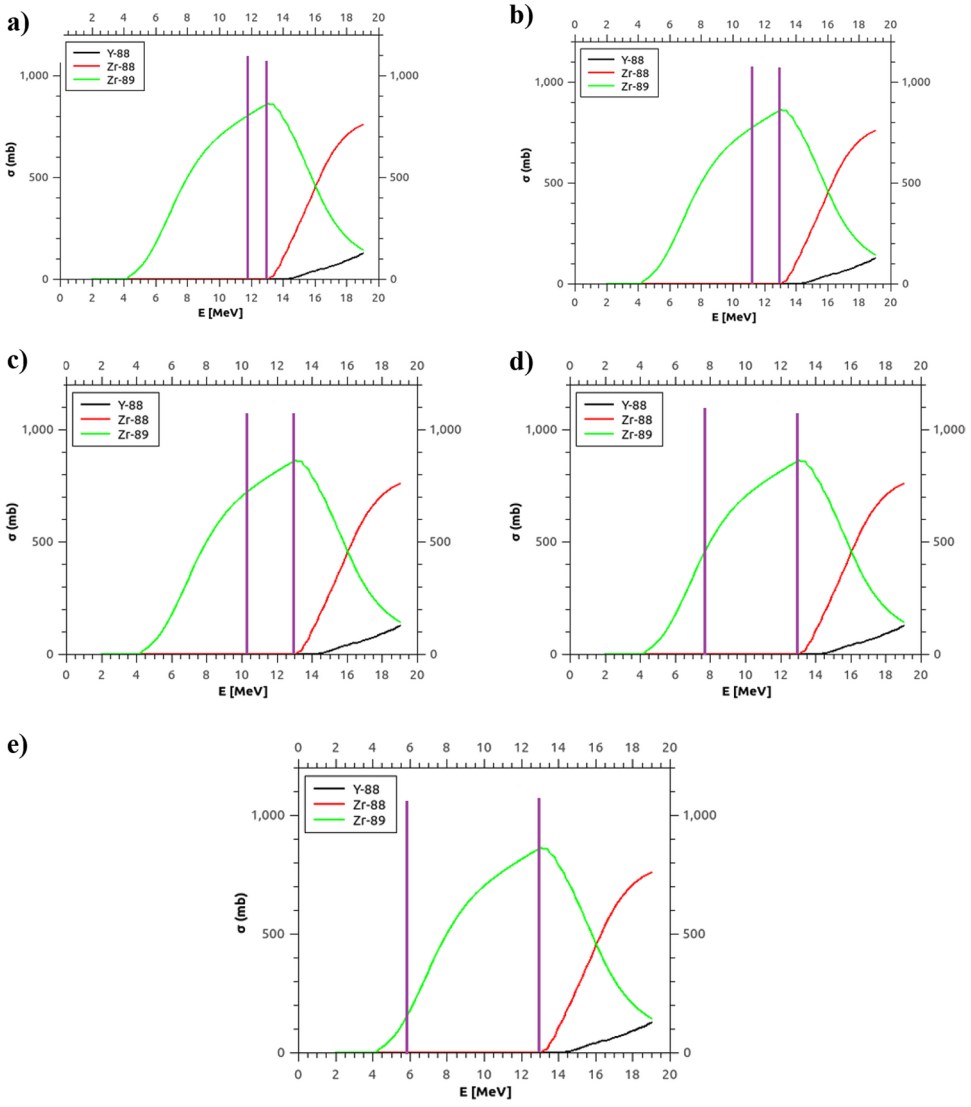

Fig. 5 The energy loss (range delimited by the two vertical purple lines) for the ^{89}Y foil thickness of: **a**) 127 µm, **b**) 150 µm, **c**) 250 µm, **d**) 500 µm, **e**) 640 µm

radioactivity is available for imaging applications, while high specific activity reduces potential side effects and improves targeting efficiency. Achieving this balance is critical for producing a clinically effective radiopharmaceutical, as it ensures adequate dose delivery with minimal non-radioactive impurities. Considering the simulation results presented in Fig. 5, we chose the yttrium foil with a thickness of 250 µm. At this thickness, protons interact efficiently with most of the yttrium atoms, ensuring high total activity of ^{89}Zr, without excessive energy loss. It also minimizes isotopic contamination and maximizes radionuclidic purity.

GEANT4 simulations

Geant4 is a software platform that uses Monte Carlo techniques to simulate how particles interact with matter [16]. It is widely applied in many fields of physics as well as in particular medical applications. The irradiation parameters which provide the best

results can be found by testing the radioisotope production parameters using the simulation tool.

Using a solid target irradiation system installed on the proton beamline extension of a TR-19 cyclotron, we simulated the nuclear reactions for the production of ^{89}Zr using Geant4. The simulation code, including its implementation and validation, was thoroughly described in our previous work [17], in which the final activity of ^{64}Cu was first calculated using the Geant4 simulation code and then produced experimentally at the Radiopharmaceutical Research Centre's TR-19 cyclotron. That study provides a detailed account of the Geant4 simulation parameters and their validation against experimental data. The input parameters used in this study to determine the activity of the radioisotope ^{89}Zr were as follows: initial beam energy, degrader thickness, energy on target, beam current, irradiation time, as well as the thickness and material of the target. As a result, the output parameters of interest were the activity at EOB and the production yield.

The experiment was conducted using the same input parameters as the simulation, and the results were compared as will be shown below.

Preparation and irradiation of the target on the ACSI solid target holder (A)

Irradiating the ^{nat}Y foils on the ACSI solid target holder that is positioned right at the cyclotron's exit will provide ^{89}Zr (Fig. 2). The target holder design with sealing Al foil, where the ^{nat}Y foil is positioned for radiation, is shown in Fig. 6. The aluminum foil covering the target support only serves the purpose of mechanically fixing the yttrium foil. The target support assembly is manually inserted through the slot visible in Fig. 6a) and its firm fixation is done by the springs also visible. The discharge of the irradiated target is done pneumatically into a lead cylinder. The focal spot is well centered and covers a big part of the surface of the 10 mm diameter target, as seen in Fig. 6b).

Considering the positioning of the yttrium foil (target) on the ACSI support shown in Fig. 7 and the minimum extraction energy of the proton beam from the cyclotron, which is 14 MeV, we determined the proton beam energy on the ^{nat}Y target using simulations. The result was an energy of 12.9 MeV, which is the energy previously determined to be optimal for having high radionuclidic purity, from the theoretical data of the main nuclear reaction shown in Fig. 3.

As can be seen in Fig. 7, the target is positioned on the sample support and sealed with aluminum foil. It is placed ahead of the cooling helium and the aluminum window at

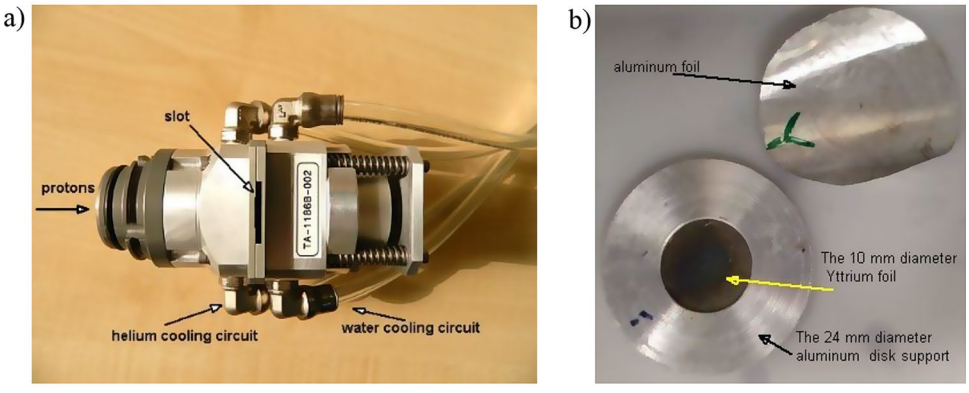

Fig. 6 **a**) ACSI solid target holder **b**) The design of the ACSI solid target holder with sealing Al foil

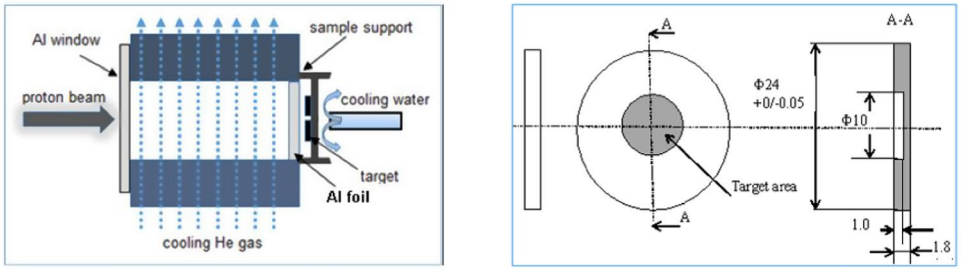

Fig. 7 Target geometry and cooling process

the proton beam's exit from the cyclotron. Figure 8 shows the energy loss of the proton beam with an energy of 14 MeV through the geometric assembly of the target, previously shown in Fig. 7.

Table 1 displays the experimental setup together with the related values and input parameters for irradiation. The thermal power dissipated during irradiation is $P = \Delta E \times I$, where ΔE is the energy degradation in the 250 μm thickness of the yttrium target and I is the proton beam current. Given the experimental conditions, it allows a cooling of maximum 20 W, so the maximum intensity will be 20 W/2.5 MeV, i.e. 8μA.

Preparation and irradiation of the target on the COMECER solid target system (B)

The dimensions of the shuttle were taken into consideration when calculating the foil's diameter for our solid target system. Also, due to the dedicated shuttle dimensions, the only thickness of the yttrium foil that can be used is 250 μm, which is also the ideal target thickness, as resulted from the simulation shown in Fig. 4c). A 50 × 50 mm foil was manually cut into a 15.5 mm diameter target with the specified thickness, and it was inserted into the dedicated shuttle. Figure 9a) shows the shuttle along with the yttrium target and the tantalum support that helds the target, Fig. 9b) shows the target fixed within the shuttle and hermetically sealed and Fig. 9c) shows the COMECER solid target unit with the shuttle being present in the irradiation position. Prior irradiation, the beam shape and position were tested using a paper burn test. The oval beam shape was fitting inside the round target surface, covering most of it.

The thermal power dissipated during irradiation in the particular case of COMECER solid target system is $P = 2.5$ MeV × 25 μA = 62.5 W. On one side of the Y foil, the helium flow will remove this thermal power, while on the other side, the contact with the water-cooled tantalum support (0.55 mm) will cool it.

The 250 μm thickness and a precisely 15.5 mm diameter target must be used to achieve an optimal heat transfer, as shown in Fig. 10.

The tool utilized to properly cut the yttrium target is shown in Fig. 11a). It includes a punch that has been carefully prepared. The two parts of the shuttle are correctly tightened using the specialized tools seen in Fig. 11b).

As previously mentioned, the minimum energy of the proton beam from the cyclotron is 14 MeV. However, on this extension line of the TR-19 cyclotron, a 320 μm aluminum degrader is mounted, which is positioned right in front of the target to be irradiated. Taking into account these parameters, according to the simulations, the energy of the protons reaching the target is 11.6 MeV, a value that is suboptimal, as can be seen in Fig. 3. Thus, the simulations varied the extracted proton beam energy within an energy range of 14–16 MeV for the 320 μm aluminum degrader in order to achieve the ideal

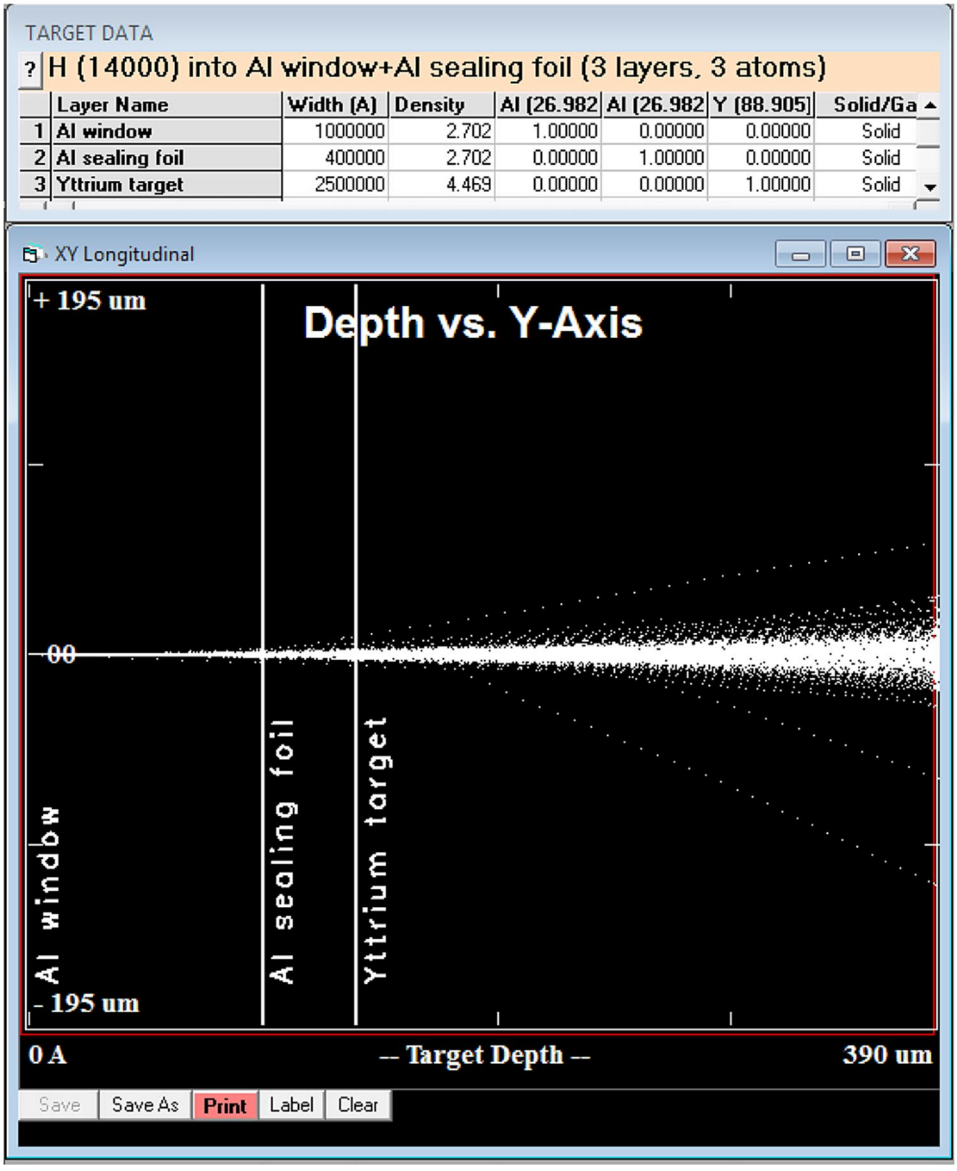

Fig. 8 The energy loss of the proton beam through the aluminum window, aluminum sealing foil and yttrium target

Table 1 Experimental configuration and input parameters for the ACSI unit

Parameters	Value
Al window	100 µm
Al foil	40 µm
^{nat}Y foil thickness	250 µm
Cooling channel - He gas	38 mm
Extracted proton beam energy	14 ± 0.3 MeV
Degraded energy reaching the target	12.9 ± 0.45 MeV
Energy at the exit of the target	10.5 ± 0.93 MeV
Beam current	8 µA
Irradiation time	4 h

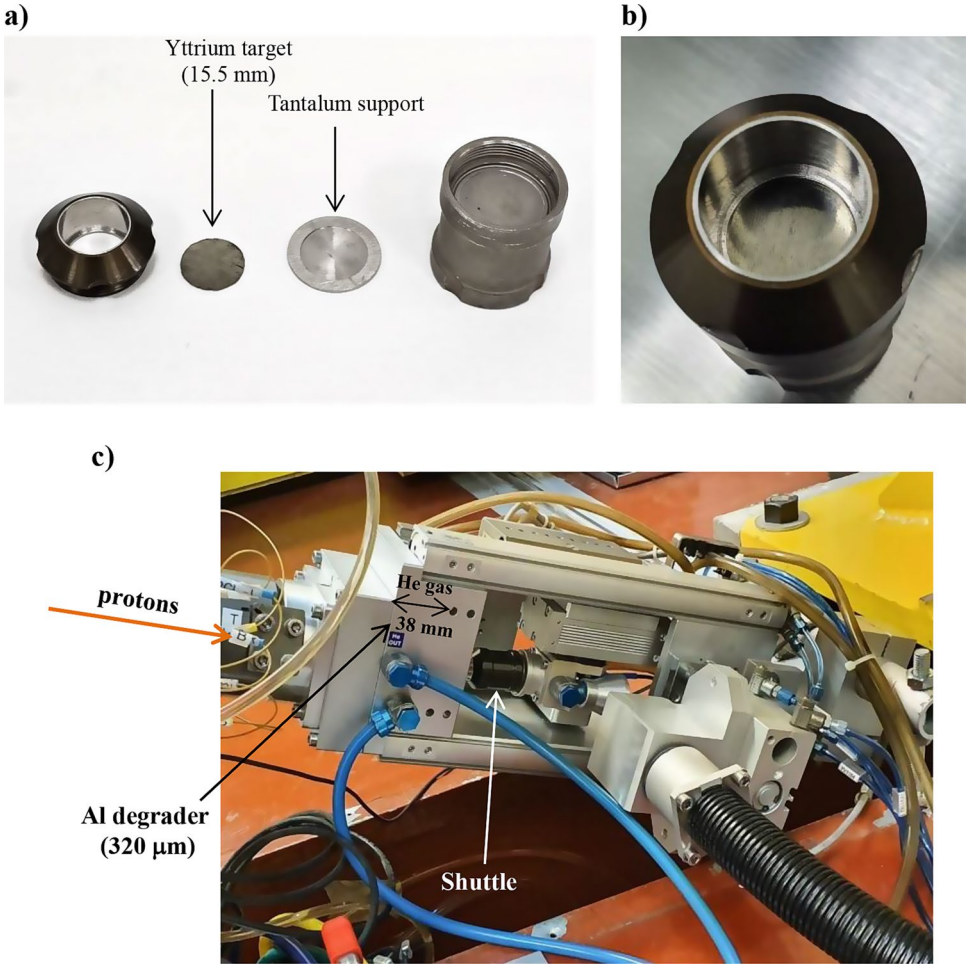

Fig. 9 **a**) the shuttle with the yttrium target and tantalum support; **b**) the target placed inside the shuttle; **c**) COMECER solid target irradiation unit

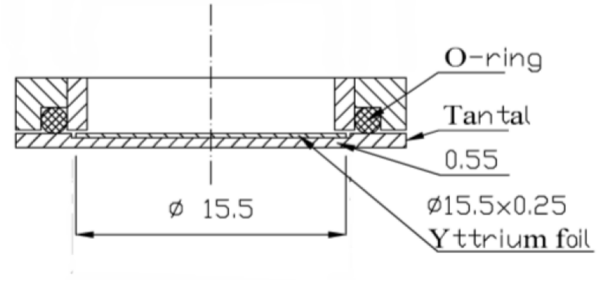

Fig. 10 Transversal section of the shuttle, with the fixing of the yttrium foil on the tantalum support (all dimensions are in mm)

proton beam energy for the highest possible production yield. The experimental setup and, implicitly, the precise location of the degrader and the target, were described in our previously published article (Baruta et al., 2022) [18]. Table 2 displays the outcomes of the SRIM/TRIM program simulations that were used to determine the exit beam energy.

The simulations provided an extracted proton energy of 15.2 MeV (±0.3 MeV broadening, i.e. the emerging cyclotron bandwidth) for the irradiation of the ^{89}Y target. By

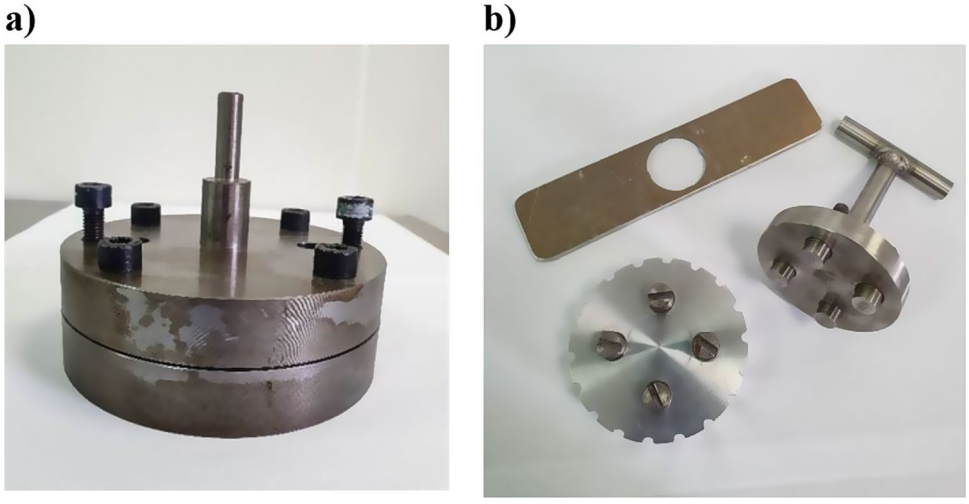

Fig. 11 **a**) The cutting device of the yttrium target, **b**) and the tools for firmly tightening the two parts of the shuttle

Table 2 The extracted and the exit proton beam energy depending on al degrader

Extracted energy (MeV)	Beam energy at the exit point (MeV)
14 ± 0.3	11.6 ± 0.64
15 ± 0.3	12.7 ± 0.67
15.2 ± 0.3	12.9 ± 0.78
15.4 ± 0.3	13.2 ± 0.76
16 ± 0.3	13.9 ± 0.68

Table 3 Experimental configuration and input parameters for the COMECER solid target system

Parameters	Value
Al degrader thickness	320 µm
^{nat}Y foil thickness	250 µm
Cooling channel – He gas	38 mm
Extracted proton beam energy	15.2 ± 0.3 MeV
Degraded energy reaching the target	12.9 ± 0.78 MeV
Energy at the exit of the target	10.4 ± 1.13 MeV
Beam current	25 µA
Irradiation time	4 h

employing aluminum foil, the proton beam energy was reduced from 15.2 ± 0.3 MeV to 12.9 MeV (± 0.78 MeV straggling).

Table 3 shows the experimental setup and irradiation parameters, based on the extracted proton beam energy, previously determined from the simulations results. The target was irradiated at the cyclotron, with a current of 25 µA, for 4 h, with a proton beam energy of 15.2 MeV.

Figure 12 illustrates the energy loss through the aluminum degrader (320 µm) and the ^{89}Y foil (250 µm), performed using the TRIM program.

Radiochemical processing of the irradiated target

The reagents used in the radiochemical processing of the final solution were purchased as follows: ultrapure hydrochloric acid, HCl, from Sigma-Aldrich (Steinheim, Germany),

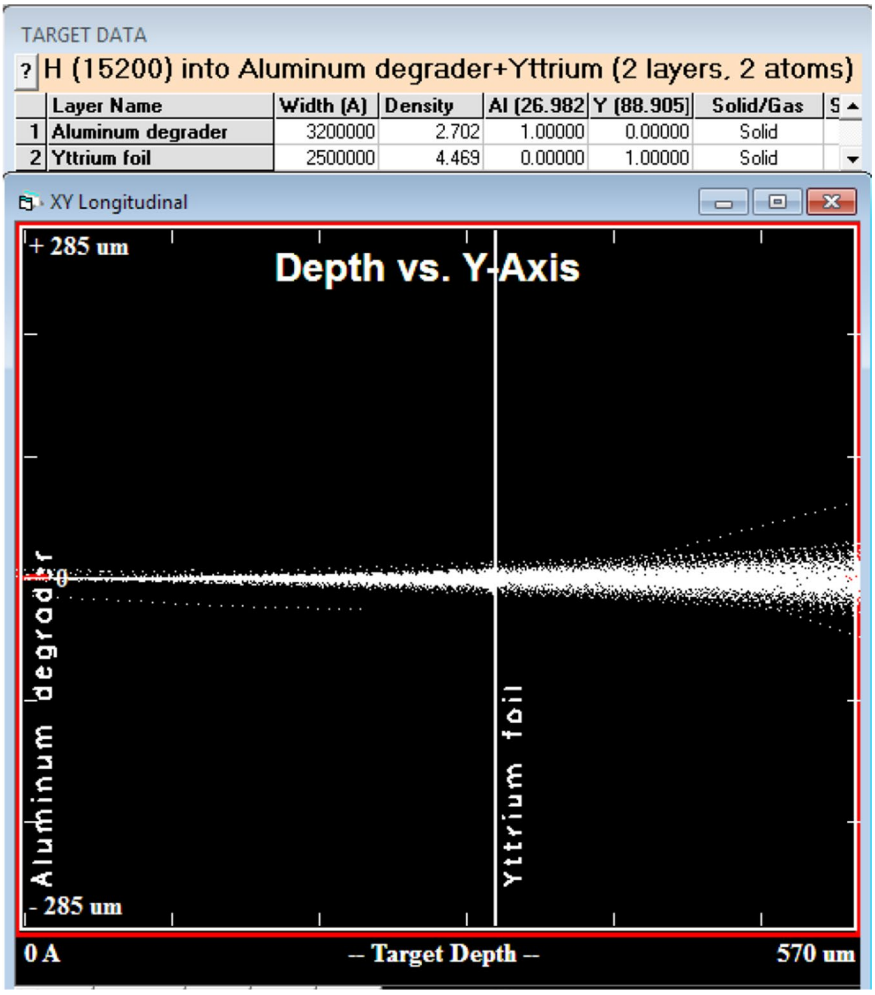

Fig. 12 The energy loss through the Al degrader and the ^{89}Y foil using TRIM

oxalic acid, 0.1 M and 1 M, from Honeywell Fluka (Muskegon, MI, USA) and ultrapure water provided by a Millipore System 8/16 (Mili-Q Direct 8, resistivity 18.2 MΩcm/25°C, TOC ≤ 5 ppb, pyrogenic impurities < 0.001 EU/mL) from Millipore SAS, France.

Following irradiation, both targets were manually dissolved in 2 M and 4 M hydrochloric acid (5 × 0.5 mL of 2 M HCl and 5 × 0.5 mL of 4 M HCl) at a temperature of 80 °C.

After 30 min of dissolution, the resulted solution was added to a specific Zr cartridge (Zr resin, Triskem, France) in order to perform the purification. We collected the impurities by washing the cartridge with 2 mL of 2 M HCl and 2 mL of water. The final solution was obtained by eluting the ^{89}Zr from the cartridge with oxalic acid (1.5 mL of 0.1 M oxalic acid and 1 mL of 1 M oxalic acid).

Characterization of the [^{89}Zr]Zr-oxalate solution

Using a gamma radiation spectrometry system with a 25% relative efficiency HPGe detector (Baltic Scientific Instruments, Latvia), a qualitative study of the [^{89}Zr]Zr-oxalate solution obtained after irradiation, dissolution, and purification was conducted. Spectral data processing was done using the InterWinner 7.0 fitting program [19].

The [^{89}Zr]Zr-oxalate solution's radiochemical purity (RCP) was assessed using a radio-TLC (ELYSIA Raytest, Germany), equipped with a BGO scintillation detector. The TLC

(thin layer chromatography) method involved the use of plastic TLC plates, silica gel coated with fluorescent indicator F254 (20 × 20 cm Merck, Darmstadt, Germany) and a mobile phase consisting of sodium citrate 0.1 M. Data processing was carried out using the GITA StarControl software [20].

Results

The experimental results obtained from irradiating the yttrium foil on the solid target holder installed on the extraction port (ACSI unit) and on the solid target irradiation system installed on the TR-19 cyclotron's extension line were in good agreement with the results of the Monte Carlo simulations for the production of ^{89}Zr via ^{89}Y(p, n)^{89}Zr nuclear reaction.

With a degraded energy of 12.9 MeV on target and an irradiation time of 4 h, the irradiation process produced an activity of 1.28 GBq ± 0.17 GBq/batch for the ACSI unit and 2.95 ± 0.25 GBq/batch EOB corrected for the COMECER unit. The proton beam currents were 8 μA and 25 μA, respectively.

Comparing the activity of ^{89}Zr resulted from the experimental work to the activity resulted within the simulations, it was observed an 18.4% difference in case of ACSI irradiation unit and a 21.3% difference in case of the COMECER irradiation unit. The results are justified by process losses during target irradiation and post-irradiation processing (dissolution and purification) and several uncertainties, such as activity measurements and cross-section values. The recovery yields were in all experiments above 92%, with a small amount of ^{89}Zr lost on the purification cartridge. The elution volume of ^{89}Zr was 2.5 mL, this resulting in a 0.7–0.85 MBq/mL at the time of measurements.

Table 4 presents the parameters of the experimental work and simulation for each production route.

The method of gamma-ray spectrometry described above was used to characterize the final solution in terms of radionuclidic purity. The sample was measured 24 h after the radiochemical processing of the irradiated target. The gamma spectrum shown in Fig. 13 indicates the characteristic peaks of the ^{89}Zr radioisotope (511, 909, 1658, 1713 and 1745 keV) with no contaminating gamma-emitting radioisotopes being identified for the 12.9 MeV proton beam energy on target. Additionally, the peak corresponding to the natural background radiation from ^{40}K (1460.8 keV) is also observed. Thus, it was confirmed the high yield of separation and the excellent radionuclide purity ≥ 99.99% of [^{89}Zr]Zroxalate purified solution, for both production routes.

The radiochemical characterization using the TLC configuration is presented in Fig. 14, where it is shown the generated spectrum and the report resulted at the end of the TLC acquisition. The radio-TLC chromatogram of the [^{89}Zr]Zr-oxalate solution shows the integrated radioactive signal for the analyzed species, the green and red area corresponding to the detected activity according to the retention factor (R/F). The total area of the signals is quantified in counts and obtained by integrating the radiochemical activity measured during the separation. This reflects the total number of pulses detected in the region of interest. The associated table provides relevant information regarding the retention factor, the percentage distribution of the activity, the type of compound analyzed and the intensity of the radioactive signal, facilitating the interpretation of the chromatographic separation.

Table 4 Input and output parameters used in simulation and experiment for production of ^{89}Zr on ACSI unit and on COMECER unit

		ACSI route to produce ^{89}Zr		COMECER route to produce ^{89}Zr	
	Input Parameters	**Simulation**	**Experiment**	**Simulation**	**Experiment**
Beam parameters	Extracted energy (from cyclotron)	14 MeV	14 MeV	15.2 MeV	15.2 MeV
	Degrader	100 µm Al window, 38 mm He cooling channel, 40 µm Al foil	100 µm Al window, 38 mm He cooling channel, 40 µm Al foil	320 µm Al foil	320 µm Al foil
	Energy on target	12.9 MeV	12.9 MeV	12.9 MeV	12.9 MeV
	Current	8 µA	8 µA	25 µA	25 µA
	Irradiation time	4 h	4 h	4 h	4 h
Target parameters	Material	^{nat}Y foil ^{89}Y 99.99%	^{nat}Y foil ^{89}Y 99.99%	^{nat}Y foil ^{89}Y 99.99%	^{nat}Y foil ^{89}Y 99.99%
	Thickness of the target	250 µm	250 µm	250 µm	250 µm
	Diameter of the target	10 mm	10 mm	15.5 mm	15.5 mm
Results	Activity at EOB	1.57 ± 0.14 GBq	1.28 ± 0.18 GBq	3.7 ± 0.39 GBq	2.95 ± 0.31 GBq
	Yield (MBq/µAh)	49 ± 4.3	40 ± 5.6	37 ± 3.9	29 ± 3.1
	Average specific activity (MBq/mg_{target})	17.8	14.5	17.1	13.6

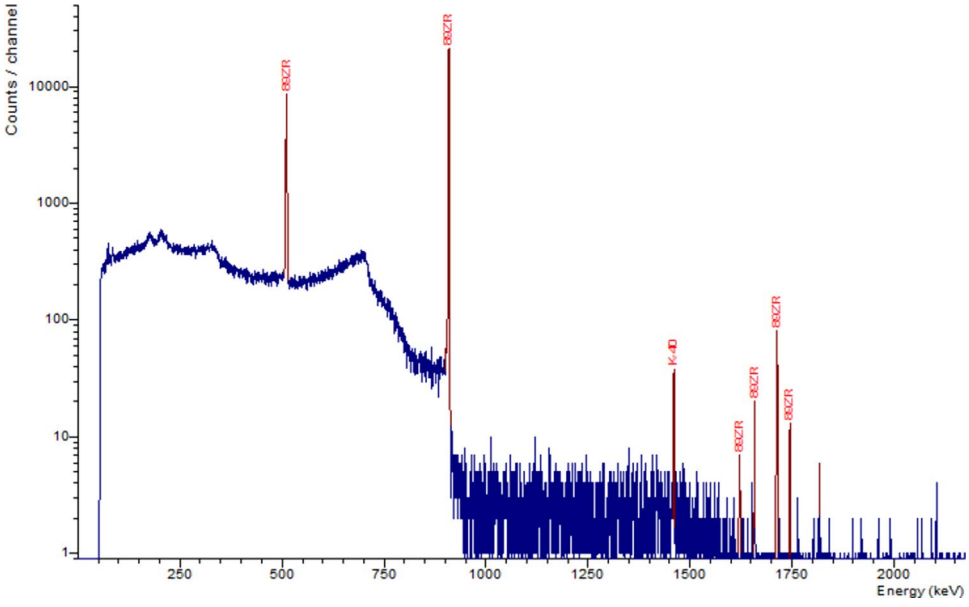

Fig. 13 Gamma spectrum of the final ^{89}Zr solution

Figure 14 shows the chromatogram resulting from the analysis of a sample of [^{89}Zr]Zr-oxalate. Given that the chromatogram shows a principal peak associated with [^{89}Zr]Zr-oxalate and a minor peak corresponding to zirconium colloid, the radiochemical purity of the solution was ≥ 95%.

In our study, we systematically varied the proton beam energy in the range of 15.2–16 MeV extracted proton beam energy (12.95–13.85 MeV on target) to evaluate the radionuclidic purity of the ^{89}Zr solution. To assess the radionuclidic purity of our ^{89}Zr samples and identify any contaminant isotopes, we analysed the gamma spectra. The

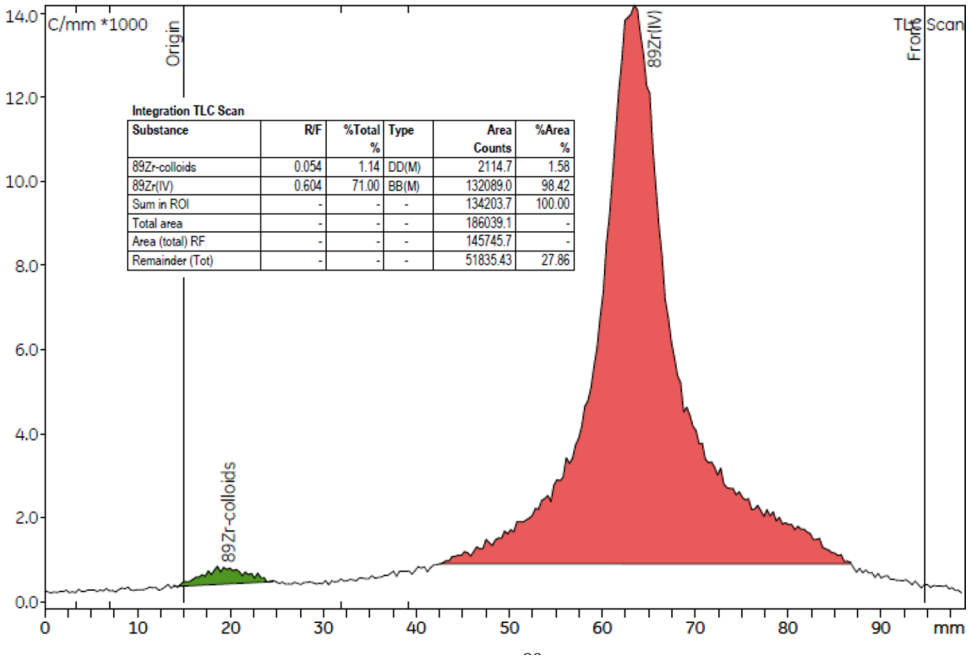

Fig. 14 Radio-TLC chromatogram of the [^{89}Zr]Zr-oxalate solution after purification

Table 5 Radionuclidic purities of ^{89}Zr and contaminants depending on the proton beam energy (mean values, $n = 5$)

Extrated energy (MeV)	Energy on target (MeV)	^{89}Zr radionuclidic purity (%)	^{88}Zr impurity (%)	^{88}Y impurity (%)	Total contaminants percentage (%)
15.2	12.95	99.99405	0.00008	0.00588	0.00595
15.4	13.17	99.99296	0.00007	0.00697	0.00704
15.8	13.63	99.99355	0.00027	0.00618	0.00645
16	13.85	99.98476	0.00071	0.01453	0.01523

samples were measured after a minimum of 5 half-lives of ^{89}Zr. The spectra enable us to observe the characteristic gamma peaks of ^{89}Zr, as well as any peaks corresponding to potential contaminants, such as ^{88}Zr and ^{88}Y. ^{89}Zr exhibits a characteristic gamma peak at 909 keV, for ^{88}Zr, characteristic peaks are observed at 392 keV, while ^{88}Y shows distinct peaks at 898 and 1836 keV.

At an energy of 12.95 MeV on target, we achieved a radionuclidic purity of 99.99% with a contaminant level (including ^{88}Zr and ^{88}Y) of only ~ 0.006%. Conversely, at a slightly higher energy of 13.85 MeV on target, the radionuclidic purity was 99.98%, with the same contaminants increasing to ~ 0.015%. The presence of a long-life contaminant as ^{88}Y (106 days) in the final solution has a substantial contribution to the radiopharmaceutical dose, even at such low percentages. These results are presented in Table 5.

Figure 15 presents the gamma spectrum obtained at 16 MeV extracted energy (13.85 MeV energy on target). It reveals the characteristic peak of ^{89}Zr alongside minor peaks from ^{88}Zr and ^{88}Y, indicating the presence of low-level contaminants at this higher energy setting.

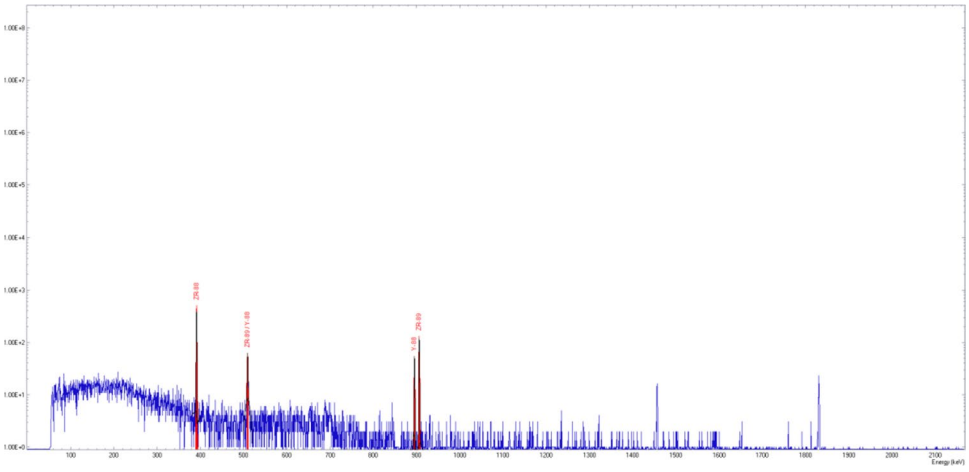

Fig. 15 Gamma spectrum for the 13.85 MeV on target

Discussions

Our study included assessments using different solid target systems, specifically irradiations with a 15.2 MeV extracted proton beam (12.9 MeV on target) with COMECER solid target system and irradiations at 14 MeV extracted energy (also 12.9 MeV on target) using ACSI solid target holder. Both systems produced comparable results in terms of radionuclidic purity and specific activity. This indicates that, at an energy of 12.9 MeV on target, both routes are effective in minimizing contaminant formation, achieving the high purity standards required for ^{89}Zr production. These findings suggest that, within this energy range, both COMECER and ACSI target systems can be used interchangeably with minimal impact on product purity and specific activity, allowing for flexible yet consistent production of ^{89}Zr.

The final activity could be improved by increasing the energy of the incident protons on the ^{89}Y target [10, 21, 22]. However, simulations and previous work have demonstrated that once the energy increases above 13 MeV, the channel for ^{88}Zr production opens, which is present as a contaminant in the final solution [23, 24]. Since it is impossible to chemically separate the contaminant ^{88}Zr from ^{89}Zr, several authors have recommended limiting the proton beam energy to a maximum of 13 MeV, preventing the formation of ^{88}Zr isotope, thereby achieving a high radionuclidic purity in the final product [3, 4, 25–29].

The variation of proton beam energy in ^{89}Zr production proved to be a critical factor in controlling radionuclidic purity and minimizing contamination from unwanted isotopes, particularly ^{88}Zr and ^{88}Y. At a lower energy setting of 12.95 MeV, we observed the highest radionuclidic purity of 99.99%, with contaminant levels held to ~0.006%. This energy level appears to be optimal for suppressing side reactions that generate isotopic impurities, allowing for a highly pure final product suitable for radiopharmaceutical applications.

In contrast, increasing the beam energy to 13.85 MeV on target resulted in a slight decrease in radionuclidic purity to 99.98%, with contaminant levels increasing to ~0.015%. This shift suggests that higher energy promotes additional nuclear reactions leading to ^{88}Zr and ^{88}Y formation. While the purity remains within acceptable limits for clinical use, even minor increases in contaminants at higher energies underscore the

importance of carefully calibrating energy settings to balance production efficiency with product purity.

These findings demonstrate the optimal purity levels in ^{89}Zr production are achieved by carefully maintaining the proton beam energy at or below 13.63 MeV on target.

Conclusions

The (p, n) nuclear reaction used in production of ^{89}Zr involves ^{89}Y as the target material, which is 100% naturally abundant and therefore reasonably priced. For the above reasons, the ^{nat}Y(p, n)^{89}Zr reaction is the most common route for the production of ^{89}Zr. However, contaminants can also be produced in a ^{nat}Y foil by the following common reactions with low positron consumption: (p, n)^{89m}Zr, (p,2n)^{88}Zr, (p, pn)^{88}Y. Fortunately, high radionuclidic purity can still be obtained using protons ~ 13 MeV, because ^{89m}Zr has a short half-life ($T_{1/2}$ = 4.2 min) and a high degree of isomeric transition (IT = 93.8%) while (p,2n) and (p, pn) reactions require higher proton beam energies.

Monte Carlo simulation of the ^{89}Zr radioisotope production agrees well with the experimental data obtained via ^{89}Y(p, n) ^{89}Zr reaction, at TR-19 cyclotron.

Our comparison of two solid target systems, COMECER and ACSI, both operating at a beam energy on target of 12.9 MeV, showed no significant differences in purity or specific activity. The [^{89}Zr]Zr-oxalate solution obtained at the end of both processes complies with technical specifications, regarding radionuclidic purity (RNP ≥ 99.99%) and radiochemical purity (RCP ≥ 95%). This similarity confirms that both target systems are effective and reliable for ^{89}Zr production, providing flexibility in system choice without compromising product quality. The purified [^{89}Zr]Zr-oxalate solution can be used as radiopharmaceutical for imaging and/or as agent for labelling antibodies, for early detection, screening and monitoring of malignant tumours, such as breast, prostate, ovarian and intestinal cancer.

Varying the proton beam energy demonstrated a clear impact on the radionuclidic purity of the ^{89}Zr production. At 12.95 MeV, the highest purity was achieved with minimal contaminant levels, suggesting this energy as optimal for suppressing unwanted isotopes like ^{88}Zr and ^{88}Y. However, at 13.85 MeV, radionuclidic purity decreased slightly, accompanied by a measurable increase in contaminants. These results meet the standard radionuclidic purity limit for radiopharmaceutical products, which requires a minimum of 99.9% radionuclidic purity to ensure patient safety and product efficacy. Our findings emphasize the importance of precise energy calibration on maximizing the purity of ^{89}Zr while minimizing the formation of unwanted isotopic impurities.

The present results offer promising perspectives for further optimization, aiming to improve the process in certain key parameters.

Abbreviations

EOB	end of bombardment
PET	positron emission tomography
CT	computer tomography
AUC	area under the curve
RNP	radionuclidic purity
RCP	radiochemical purity
TLC	thin layer chromatography
SRIM	the Stopping and Range of Ions in Matter software package
TRIM	the Transport of Ions in Matter program

Acknowledgements

Access to TR-19 Cyclotron facility was granted under IOSIN program of the Romanian Ministry of Research, Innovation and Digitization.

Author contributions
Conceptualisation, D.N., D.C. and S.B.; methodology, D.C., S.B., R.L., A.N. and M.-R.T.-C.; software, S.B., A.N. and M.-R.T.-C.; analytical methods, S.B., A.N. and M.-R.T.-C; investigation, D.C. and S.B.; irradiation L.C.; data curation, D.C.; writing-original draft preparation, D.C., S.B. and M.-R.T.-C.; writing-review and editing, D.N., L.C., R.L. and A.J.; supervision, D.N. and L.C.; project administration, D.N.

Funding
This work was supported by PN23210201 and IAEA CRP F22071, Contract 23375.

Data availability
The data and materials are available on reasonable request to the corresponding author.

Declarations

Ethics approval and consent to participate
Not applicable.

Consent for publication
All authors have read and agreed to the published version of the manuscript.

Competing interests
Authors declare no conflict of interest concerning the submitted work.

Received: 10 December 2024 / Accepted: 18 April 2025
Published online: 12 May 2025

References

1. Kasbollah A, Eu P, Cowell S, Deb P. Review on production of 89Zr in a medical cyclotron for PET radiopharmaceuticals. J Nucl Med Technol. 2013;41(1):35–41.
2. Tateishi U, Daisaki H, Tsuchiya J, Kojima Y, Takino K, Shimada N, Yokoyama K. Image quality and quantification accuracy dependence on patient body mass in 89Zr PET/CT imaging. EJNMMI Phys. 2021;8(1):1–11.
3. Bhatt NB, Pandya DN, Wadas TJ. Recent advances in zirconium-89 chelator development. Molecules. 2018;23(3):638.
4. Queern SL, Aweda TA, Massicano AVF, Clanton NA, El Sayed R, Sader JA, Lapi SE. Production of Zr-89 using sputtered yttrium coin targets. Nucl Med Biol. 2017;50:11–6.
5. Nuclear Data Search (n.d.). Accessed on December 5, 2024. http://www.lnhb.fr/Laraweb/
6. ACSI. Advanced cyclotron systems Inc. (ACSI). 2003. [Online]. Available at: http://www.advancedcyclotron.com/cyclotron-solutions/tr19
7. Ursu I, Craciun L, Niculae D, Zamfir NV. The radiopharmaceuticals research centre of IFIN-HH at start. Rom J Phys. 2013;58:1327–36.
8. Leonte RA, Niculae D, Crăciun LS, Căta-Danil G. Medical radioisotopes production at TR -19 cyclotron from IFIN-HH. UPB Sci Bull Ser A: Appl Math Phys. 2017;79:223–36.
9. ALCEO. Solid target processing system (ALCEO). 2019. [Online]. Available at: https://www.comecer.com/alceo-solid-target-processing-system
10. Sharifian M, Sadeghi M, Alirezapour B, Yarmohammadi M, Ardaneh K. Modeling and experimental data of zirconium-89 production yield. Appl Radiat Isot. 2017;130:206–10.
11. Koning AJ, Hilaire S, Duijvestijn MC. (2007). TALYS-1.0. In *International Conference on Nuclear Data for Science and Technology* (pp. 211-214). EDP Sciences.
12. Koning AJ, Rochman D, Sublet JC, Dzysiuk N, Fleming M, Van der Marck S. TENDL: complete nuclear data library for innovative nuclear science and technology. Nucl Data Sheets. 2019;155:1–55.
13. Mustafa MG, West Jr HI, O'brien H, Lanier RG, Benhamou M, Tamura T. Measurements and a direct-reaction–plus–Hauser-Feshbach analysis of Y 89 (p, n) 89 Zr, Y 89 (p, 2n) 88, and Y 89 (p, pn) 88 Y reactions up to 40 mev. Phys Rev C. 1988;38(4):1624.
14. EXFOR. Experimental nuclear reaction data (EXFOR). 2023. [Online]. Available at: https://www-nds.iaea.org/exfor/
15. Team MC. MCNP5/MCNPX-exe package, Monte Carlo N-particle extended. Los Alamos National Laboratory report; 2008.
16. F. Ziegler J. SRIM-2003. Nucl Instrum Methods Phys Res Sect B. 2004;219:1027–36.
17. Agostinelli S et al. Geant4 - a simulation toolkit. Nucl Instrum Methods Phys Res A, pp. 250–303, 2003.
18. Baruta S, Leonte R, Cocioaba D, Craciun L, Ur CA, Niculae D. (2022) Cyclotron production of ^{64}Cu by proton irradiation of enriched ^{64}Ni target: Validation of Geant4 simulation parameters through experimental data. *Front. Phys.* 10:1038014. doi: 0.3389/fphy.2022.1038014.
19. InterWinner, [Online]. Available: https://www.itech-instruments.com/InterWinner.pdf
20. Radiopharmaceutical Quality Control Instruments. (n.d.). Accessed on December 5, 2024. https://www.elysia-raytest.com/assets/4fca4ea4-7196-4b17-8314-5e5e719eb8bb/flw-027-minigita.pdf
21. Holland JP, Sheh Y, Lewis JS. Standardized methods for the production of high specific-activity zirconium-89. Nucl Med Biol. 2009;36(7):729–39.
22. Pandey MK, Bansal A, Ellinghuysen JR, Vail DJ, Berg HM, DeGrado TR. A new solid target design for the production of 89Zr and radiosynthesis of high molar activity [89Zr] Zr-DBN. Am J Nucl Med Mol Imaging. 2022;12(1):15.
23. Jalilian AR, Osso JA. Production, applications and status of zirconium-89 ImmunoPET agents. J Radioanal Nucl Chem. 2017;314:7–21.
24. La MT, Tran VH, Kim HK. Progress of coordination and utilization of zirconium-89 for positron emission tomography (PET) studies. Nuclear Med Mol Imaging. 2019;53:115–24.

25. Dabkowski AM, Probst K, Marshall C. (2012, December). Cyclotron production for the radiometal Zirconium-89 with an IBA cyclone 18/9 and COSTIS solid target system (STS). In *AIP Conference Proceedings* (Vol. 1509, No. 1, pp. 108-113). American Institute of Physics.
26. Dabkowski A, Paisey S, Talboys M, Marshall C. Optimization of cyclotron production for radiometal of zirconium 89. Acta Phys Pol A. 2015;127(5):1479–82.
27. Wang, F., Ding, J., Guo, X., Liu, T., Ding, L., Xia, L.,… Yang, Z. (2021). Production of the next-generation positron nuclide zirconium-89 (89Zr) guided by Monte Carlo simulation and its good quality for antibody labeling. Journal of Labelled Compounds and Radiopharmaceuticals, 64(1), 47-56.
28. Infantino, A., Cicoria, G., Pancaldi, D., Ciarmatori, A., Boschi, S., Fanti, S.,…Mostacci, D. (2011). Prediction of 89Zr production using the Monte Carlo code FLUKA. Applied Radiation and Isotopes, 69(8), 1134-1137.
29. Tang, Y., Li, S., Yang, Y., Chen, W., Wei, H., Wang, G.,… Liu, N. (2016). A simple and convenient method for production of 89Zr with high purity. Applied Radiation and Isotopes, 118, 326-330.

Publisher's note